*Int. J. Therm. Sci.* (2001) 40, 738–752

S1290-0729(01)01262-5/FLA

# A thermographic method to map the local heat transfer coefficient on the complete surface of a circular cylinder in an airflow

Laetitia Ghisalberti, Alain Kondjoyan *

*Equipe Génie des Procédés, Station de Recherche sur la Viande, INRA, 63122 Staint Genès Champanelle, France*

(Received 28 April 2000, accepted 17 October 2000)

**Abstract** — A constant wall heat flux method was developed to map the transfer coefficient value at the surface of a circular cylinder whose height to diameter ratio was 3. The cylinder was positioned either cross-flow or sloped at 45° into the flow. Preliminary experiments showed that the heat flux had to be generated nearly all over the body to avoid surface conduction which meant it was difficult to make the sample. The surface temperatures were measured by an infrared camera which was located outside the experimental cell to avoid flow disturbances. Procedures were developed to be able: (i) to the get infrared pictures through a window and (ii) to rebuild from these pictures and without distortion the complete distribution of the heat transfer coefficient at the surface of the cylinder. © 2001 Éditions scientifiques et médicales Elsevier SAS

**heat / transfer / coefficient / air / cylinder / map making**

## Nomenclature

| | | |
|---|---|---|
| $Bi$ | Biot number $= h \cdot L/\lambda$ | |
| $C_i$ | constants used in relation (2) and (3) | |
| $D$ | cylinder diameter . . . . . | m |
| $e$ | thickness in which surface conduction occurs (2) . . . . . | m |
| $H$ | cylinder height . . . . . | m |
| $h$ | heat transfer coefficient . . . . . | $W \cdot m^{-2} \cdot K^{-1}$ |
| $K$ | constant used in relation (2) and (3) | |
| $L$ | characteristic dimension of the product . | m |
| $r$ | major to minor axis ratio of an elliptical cylinder | |
| $T_s$ | temperature at the surface of the cylinder | °C or K |
| $T_{air}$ | air temperature . . . . . | °C or K |
| $Tu$ | turbulence intensity in the main flow direction: $\frac{\sqrt{\overline{u^2}}}{U_\infty}$ . . . . . | % |
| $u$ | velocity fluctuation around $U$ . . . . . | $m \cdot s^{-1}$ |
| $U$ | mean air velocity in the flow direction . | $m \cdot s^{-1}$ |
| $X$ | curvilinear distance along the cylinder from the stagnation point . . . . . | m |
| $y$ | distance from the bottom guard heater in the cross-flow direction . . . . . | m |

*Greek symbols*

| | | |
|---|---|---|
| $\varepsilon$ | emissivity of the cylinder surface | |
| $\Phi$ | heat flux at the wall . . . . . | $W \cdot m^{-2}$ |
| $\Delta$ | difference of temperature between the guard heaters and the middle line of the measurement area . . . . . | °C |
| $\theta$ | angle from the stagnation point of the cylinder . . . . . | degree |
| $\lambda$ | thermal conductivity of the product, of the sample or of the wire . . . . . | $W \cdot m^{-1} \cdot K^{-1}$ |
| $\sigma$ | Stefan–Boltzmann constant . . . . . | $W \cdot m^{-2} \cdot K^{-4}$ |

*Mean*

| | |
|---|---|
| $\overline{x}$ | mean of $x$ |

## 1. INTRODUCTION

Many industrial processes are based on a simultaneous heat and water transfer between a solid of complex shape and an air flow. This is often the case for food processes such as chilling, drying, cooking or freezing. As soon as

* Corrrespondence and reprints.
*E-mail address:* alain.kondjoyan@clermont.inra.fr (A. Kondjoyan).

the air velocity is greater than 0.4–0.5 $m \cdot s^{-1}$, exchanges by convection are preponderant. Mean fluxes exchange by convection at the surface of the product can be calculated if the average values of the transfer coefficients are known. These mean transfer coefficients result from the integration of local values which can be very different from one point of the body surface to the other. In some cases, the knowledge of the distribution of the transfer coefficients can be of direct practical interest. For example, it serves to predict the risks of deterioration at the surface of the product during intense chilling or heating treatments (very fast chilling, re-heating or cooking). It is also interesting to know the distribution of the transfer coefficient to explain the variation of its average value which depends on many factors: velocity and turbulence of the flow, shape, dimensions and position of the product. A lot of experiments are needed to take into account the effect of all these factors. Interpretations based on the local variations of the transfer coefficient could help reducing the number of experiments.

During a simultaneous heat and water exchange between a water saturated product and an air flow, the relation of Lewis applies. The mass transfer coefficient value is proportional to the heat transfer coefficient. Thus the distribution of one of these coefficients gives the distribution of the other. This study aims at developing a method to map the local heat or mass transfer coefficient value at the complete surface of a product.

## 2. BIBLIOGRAPHY

The main methods used in the field of food engineering to measure the average transfer coefficient value have been listed by Arce and Sweat [1]. To our knowledge no work has been performed to list the different methods used to measure the local transfer coefficient values.

The different methods used in the literature fall into three categories: those that determine the mass transfer coefficient alone, others that determine the heat transfer coefficient alone and those that determine simultaneously both of them.

Methods that enable the simultaneous determination of the heat and mass transfer coefficients are mostly steady-state methods based on the evaporation of substances such as water [2, 3], benzene [4] or nitrobenzene [5]. Usually, it is not possible with these methods to determine the local transfer coefficient values since it would be necessary to measure the local amount of product which evaporates, which is technically very difficult. However, an adaptation of the "psychrometric" method has been performed in the laboratory to determine some of the local transfer coefficient values on products of very complex shapes [2, 6, 7]. But it requires very precise measurements of the surface temperatures, it remains punctual and is restricted (for local determinations) to air velocities lower than 1.0 $m \cdot s^{-1}$.

### 2.1. Mass transfer coefficient

Methods which enable a local determination of the mass transfer coefficient in air are mostly based on the sublimation of a substance, often *Naphthalene*, which covers the surface of the sample. The substance to be sublimated should be applied regularly on the surface, which is already difficult when the shape of the sample is elementary and is particularly laborious if the shape is a little more complex.

During the experiment, weight losses and variations in the thickness of the substance are very small. This leads to large uncertainties in determining the results. For example, Kestin and Wood [8] mentioned a $\pm 8\%$ error in determining the coefficient due to the precision of the measurements. This 8% error is probably the minimum that one can expect using this type of method. If these experiments are repeated, the local differences in thickness of the sublimated substance change progressively the shape of the sample [9]. Thus the sample has to be frequently rebuilt [10], which is in practice very cumbersome.

Because of all these difficulties, such methods cannot be easily used to map the transfer coefficient value at the complete surface of samples whose shape is not elementary. Moreover, because of the large number of potential biases, such methods are commonly considered less accurate than those based on the determination of the heat transfer coefficient [9].

### 2.2. Heat transfer coefficients

#### Transient methods

The different methods used to determine the heat transfer coefficient can be divided into steady-state methods and transient methods, depending on their conditions of application.

Transient methods consist in heating or cooling a sample whose heat conductivity is known perfectly. The heat transfer coefficient values are determined by measuring the temperature kinetics at the surface of the product.

When the Biot number is very small $Bi < 0.1$ (sample of small dimensions and high heat conductivity), the temperature is uniform everywhere at the surface and inside the sample. In this case only the average transfer coefficient can be determined.

Some experiments have also been performed with Biot numbers much greater than 0.1 (sample built in a very insulating material) [11–13]. In this case, it is theoretically possible to obtain the distribution of the transfer coefficient values if the temperature kinetics at the body surface are measured and if the exchanges by conduction inside the sample can be calculated under transient conditions. When the shape of the sample is elementary (flat plate, infinite circular cylinder, sphere), the exchanges by conduction can be considered as unidirectional and analytical solutions can be found in the literature. When the shape of the body is not elementary, these analytical solutions cannot be applied directly. In some simple cases, it is possible to fit them using correcting factors named "shape factors" [11, 13]. In other cases, the exchanges by conduction inside the product have to be solved numerically [14, 15]. In these cases, transfer coefficients are not really calculated but fitted to mimic the evolution of the surface temperatures. This procedure can become very difficult to apply if the shape of the sample is complex.

### Steady-state methods

These are constant wall heat flux methods. To obtain the distribution of the heat transfer coefficient, the heating element must be positioned at the surface of the sample and be directly in contact with air. The local value of the transfer coefficient is very easily calculated from the power supplied to the heating element (heated most of the time electrically) and the local difference in temperature between the body surface and air.

When the shape of the sample is symmetrical, two types of experimental techniques can be used. For a sphere or an infinite circular cylinder, the heating element can cover only a tiny part of the surface which is moved afterwards to obtain the distribution of the transfer coefficient on a line [16]. In the other cases (elliptical cylinder, etc.) the heating element, usually a ribbon, covers a large part of the body surface.

Although it is theoretically simple to determine the distribution of the transfer coefficient by a constant heat flux method, its application is difficult because of the exchanges due to conduction.

Exchanges by conduction can take place at the body surface from the heated area to the non heated area and when a heating ribbon is used inside the ribbon itself. The effects of conduction inside a ribbon have not been considered in the literature. To decrease the conduction from the heated to the non heated area, one could consider decreasing considerably the heating power. However that tends to decrease the accuracy in determining the heat transfer coefficient [16–18]. The best solution is probably to reduce the difference in temperature between the measurement and non measurement area. The ribbon can be sandwiched between two guard heaters [19] or, for tiny heating elements, more complicated devices can be used [20].

Another simpler solution is to use a very large ribbon and to determine the transfer coefficients only on the middle line of the ribbon where the exchanges by conduction are negligible. However this technique cannot be applied to map the transfer coefficient value all over the surface of the body.

### Temperature measurements at the surface of the sample

Temperature measurements at the surface of the sample are needed to determine the local heat transfer coefficients. When the sample shape is elementary, only a few thermocouples are necessary. As soon as the shape of the sample is more complex, the number of thermocouples has to be increased to properly describe the distribution of the transfer coefficient. For example, Ota et al. [21] placed 49 thermocouples on the middle line of an elliptical cylinder of axis ratio $r = 2$. Measuring the temperatures on several lines of the body surface using thermocouples quickly becomes unfeasible. To cope with this difficulty, some authors have covered the sample with liquid crystals which colour changes with temperature [22, 23]. Surface temperature can also be measured using infrared pyrometers or a camera [24, 25]. However this technique is seldom used to determine transfer coefficients [26].

## 3. THE METHOD AND ITS LIMITS DUE TO CONDUCTION

### 3.1. Principle

Following the previous analysis, the heat transfer coefficient was determined rather than the mass transfer coefficient. A constant heat flux method which is a method of reference was preferred to a transient method to avoid numerical calculations of exchanges by conduction and transfer coefficient fitting. Surface temperatures

were measured using an infrared camera (type TVS 2100 MKII of Nippon Avionics Corporation) which was available at the laboratory.

The method was tested on a circular cylinder ($D = 0.1$ m) whose height to diameter ratio $H/D$ was 3.0. The cylinder was placed either cross-flow or sloped with a 45° angle into the flow. The cylinder was supported by a threaded rod fixed to its bottom end. Apart from this rod, the ends were left free in the stream.

The aim of the study was to map the heat transfer coefficient all over the cylinder surface, that is on its side as well as on its ends (hereafter called tips). In this case, the classic heating ribbon technique cannot be used to cover both the side and tips. Thus the ribbon was replaced on the tips by an oxy-insulated electrical wire which can be contiguously coiled to cover the whole surface. Ribbons could have been used on the cylinder side. However we were not able to find ribbons which had exactly the same characteristics as the wire (electrical and thermal conductivities, nature of the surface and thickness). Thus to avoid any bias, we decided to also coil the side of the cylinder using the same wire as for the tips.

During the experiments, the sample was located inside the experimental cell (0.8 m × 0.8 m × 1.60 m) of a wind tunnel which has already been described elsewhere [2, 6, 7]. The air velocity ranged from 0.5 m·s$^{-1}$ to 5.0 m·s$^{-1}$ and the air temperature was close to 25 °C. The air temperature was precisely measured near the sample using PT100 probes.

To avoid flow disturbances, the infrared camera was located outside the experimental cell. Thus, surface temperatures had to be measured through a window fixed up in one of the cell walls.

When a constant heat flux is generated at a solid surface and when the steady-state period is reached, the heat transfer coefficient $h$ can be directly determined from the energy balance by:

$$h = \frac{\Phi}{T_s - T_{air}} - \varepsilon\sigma \frac{T_s^4 - T_{air}^4}{T_s - T_{air}} \qquad (1)$$

(I) (II)

Term (I) describes the transfer by convection and (II) the transfer by radiation. $T_s$ and $T_{air}$ are the surface and air temperature (expressed in Kelvin), respectively; $\varepsilon$ is the emissivity of the solid, $\sigma$ the Stefan–Boltzmann constant.

A quick look at relation (1) proves that the smaller the difference $T_s - T_{air}$ is, the greater the effect of an error in the temperature measurements is on $h$. It was difficult to measure the surface temperatures by the infrared camera with an error less than ±0.5 °C. Thus the temperature at the surface of the sample should be at least 35–40 °C higher than the air temperature to ensure a precision of 3% on the determination of the heat transfer coefficient. As the air temperature was about 25 °C, the surface of the cylinder must be heated to 60 °C–75 °C.

It is assumed in relation (1) that all the heat flux is dissipated by convection and radiation and that the differences in surface temperature are only due to the local variations of the heat transfer coefficient. This is never fully verified in practice since there are some exchanges by conduction: (1) inside the electrical wire and (2) at the body surface from the heated to the non (or less) heated area. The conduction from the surface to the inside of the sample will not be discussed here because it was found to be negligible as soon as the steady-state period was reached.

To ensure the accurate determination of the local value of the transfer coefficient at the body surface, the previous exchanges by conduction should be taken into account.

### 3.2. Temperature equalisation inside the electrical wire

The electrical conductivity of the wire must be high enough to be able to heat the surface of the sample. However high electrical conductivity goes most often with high thermal conductivity. A wire made in Nickel–Chrome was used which seemed to be a good compromise between good electrical conductivity and low thermal conductivity (60% Nickel and 15% Chrome, $\lambda = 13$ W·m$^{-1}$·K$^{-1}$, wire diameter 0.8 mm). It was oxy-insulated and could be coiled continuously wire against wire.

Even if the thermal conductivity of Nickel–Chrome is small, there is an unavoidable heat exchange by conduction that tends to homogenise the surface temperature.

As no wire with a lower thermal conductivity than that of the Nickel–Chrome was available, it was not possible to study experimentally the effect of conduction inside the wire on the distribution of the heat transfer coefficient. Thus the distribution of the heat transfer coefficients at the surface of a circle covered with a wire was simulated numerically using the software “Fluent”. The circle was 0.1 m in diameter and the thermal conductivity and diameter of the wire were those of the Nickel–Chrome used during the experiments. No transfer by conduction existed from the surface toward the centre of the circle. The amount of heat generated by the wire

which was dissipated by convection led to differences in temperature at the body surface comparable with those which existed under practical conditions. During calculations, the air velocity was 1.0 $m \cdot s^{-1}$ and the turbulence intensity 20%. These conditions were chosen since they speed up the convergence of calculations while the resulting transfer coefficient values were close to the practical ones. However one should not wait here for a realistic determination of the effect of the 3-dimensional turbulence on the heat transfers around a wire loop. Some of the difficulties to assess the effect of turbulence by 2-dimensional calculations have already been discussed in a previous paper [27].

During the present calculations, the heat flux was fixed in order that the temperature, which varied at the solid surface due to the local difference in the heat transfer coefficient, was near 70 °C. The air temperature was 20 °C. Flow modelling and numerical procedures are not described here. They were identical to the ones used previously by Kondjoyan and Boisson [27]. Thermal calculations were performed under two conditions: with and without exchanges by conduction inside the wire.

The distributions of the heat transfer coefficient obtained under both types of conditions are compared in *figure 1*. The distributions of the coefficient calculated using "Fluent" were not exact but sufficiently realistic to be able to quantify the effect of conduction. Conduction tends to heat the part of the surface located upstream from the separation point and to cool the part which is downstream. The consequence of this phenomenon is much more pronounced in the wake because as the convection is smaller, the proportion of the total energy exchanged by conduction is greater. This phenomenon is inherent to the method and tends to smooth the variations of the heat transfer coefficient in the regions where flow separation and reattachment occur. However when a Nickel–Chrome wire is used, the magnitude of the errors remains moderate and cannot question the use of the constant heat flux method.

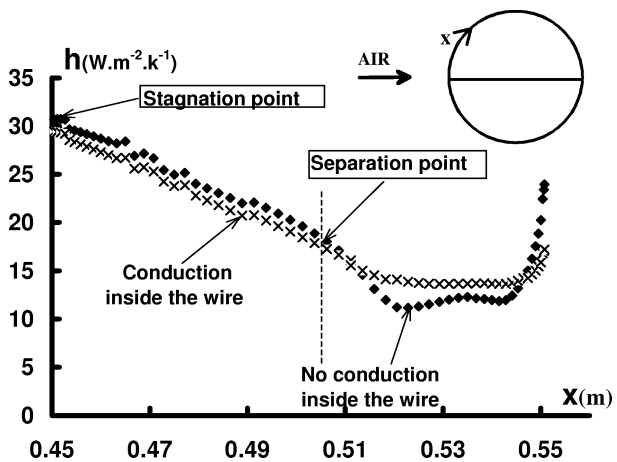


**Figure 1.** Distribution of the heat transfer coefficient values calculated using the software "Fluent" at the surface of a circular cylinder 0.1 m in diameter, covered by Nickel–Chrome wire. The distribution was calculated under two conditions: (1) with conduction inside the wire and (2) without conduction. $X$ corresponds to the distance in the flow direction along the surface of the circle.

## 3.3. Effects of conduction at the edges of the heated area

Initially, we had thought of applying the constant heat flux method by coiling the wire only on a reduced area of the cylinder side and then moving this area at the surface of the sample. This procedure would have lightened the technical work of coiling the wire on the cylinder side and would have enabled the use of cheaper equipment (in particular less powerful electrical generators). But the procedure raised an important question: how much would the conduction at the edges of the heating area affect the results? Preliminary experiments were conducted on the cylinder in cross flow to answer this question.

The cylinder was hollow (0.1 m in diameter), made in polypropylene ($0.8 \cdot 10^{-3}$ m in thickness) and filled with glass wool. Polypropylene is a thermal insulated material which resists temperatures up to about 100 °C without deformation. The device was made of three main pieces which fitted into each other. On the middle piece, 47 loops of the Nickel–Chrome wire were coiled continuously which spanned 0.04 m of the cylinder surface. This measurement area was sandwiched between two guard heaters each made of 12 loops of the Nickel–Chrome wire. Each of the guard heaters has a separate electrical supply. To prevent short circuits, a loop of a varnished copper wire—which was not electrically supplied—separated each of the guard heaters from the measurement area. This middle piece built was sandwiched between two hollow polypropylene tubes. These tubes were filled with glass wool and had a lid on.

The last stage in making the sample aims at making the surface of the cylinder, and particularly the coil, flat, smooth and as opaque as possible ($\varepsilon$ close to 1). Several fin coats of cellulose filler were applied with a brush. Then the surface was sanded down and covered with three coats of a mat black painting which could resist high temperatures.

At the beginning of an experiment, the voltage and electrical intensity through the measurement area were

fixed according to the experimental conditions ($U$, $Tu$) to reach an average temperature at the surface of the sample between 60 °C and 80 °C. Then the voltage and electrical intensity through each of the guard heaters (separate electrical supplies) were fitted to obtain temperature values close to the temperature which existed on the middle line of the measurement area. As on a wire loop, the temperature changed in the flow direction, it was possible either to fit the temperature at the stagnation point where the value was minimum or at the separation point were it was maximum. If the temperatures of the guard heaters were fitted at the stagnation point, then the measurement area tended to be cooled in the wake. On the contrary, if the temperatures were fitted at the separation point then the measurement area was heated at the stagnation point. Heating the measurement area altered the results in a way which was more difficult to quantify. Thus we preferred to fit the temperatures at the stagnation point and then to analyse the effect of conduction on the distribution of the transfer coefficient in the wake. This effect was analysed by varying at the stagnation point the difference in temperature between the guard heaters and the middle of the measurement area. Five experiments were performed with an air flow velocity of 0.5 m·s$^{-1}$, that is in the case for which the exchanges by conduction were the greatest. The differences in temperature at the stagnation point between the guard heaters and the middle of the measurement area $\Delta$ were: $-4.0$ °C, $-2.0$ °C, $-0.5$ °C, $-1$ °C, $+1$ °C, $+2$ °C. In the wake, differences were $+3.0$ °C to $+5.0$ °C greater.

These experiments were completed by calculations based on the resolution of the energy balance at the cylinder surface. When there is no exchange by radiation the profile of temperature can be directly determined using an analytical solution of literature [28]:

$$T_y - T_{\text{air}} = -\left[C_2 e^{-my} + C_3 e^{my}\right] \qquad (2)$$

with: $m = \sqrt{\frac{h}{K}}$ and $K = \lambda \cdot e$. $y$ is the distance in the cross flow direction, $h$ the heat transfer coefficient, $\lambda$ the conductivity of the solid and $e$ the thickness in which surface conduction exchange occurs.

During our calculations relation (2) was modified in relation (3) to account for radiation:

$$T_y - T_{\text{air}} = \frac{\Phi - C_1}{K \cdot m^2} - \left[C_2 e^{-my} + C_3 e^{my}\right] \qquad (3)$$

where $C_1$ is a constant which permit to linearized the term of radiation in a small range of temperatures.

Details on the determination of $C_1$, $C_2$ and $C_3$ from the boundary conditions and on the resolution procedure can be found in publication [29].

The experimental profiles of temperature measured in the cross-flow direction of the vertical cylinder showed the increase of temperature from the guard heaters to the middle line of the measurement area. A typical profile obtained at the stagnation point for a difference $\Delta$ of $-4$ °C in temperature between the lower guard heater and the center of the measurement area is presented in *figure 2*. In this figure the distribution appears to

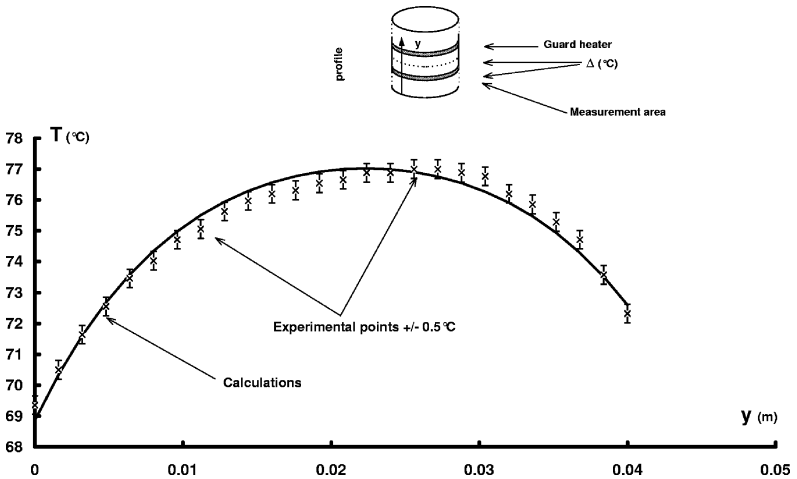


**Figure 2.** Preliminary experiments on a small heated measurement area located at mid-height of the side of the cylinder and sandwiched in between two guard heaters. Cross profiles of the temperature at the stagnation point of the cylinder for a difference $\Delta$ of 4 °C between the guard heaters and the middle of the measurement area. $y$ is the distance in the cross flow direction from the bottom guard heater to the top. Symbols represent the experimental points, full line results from calculations.

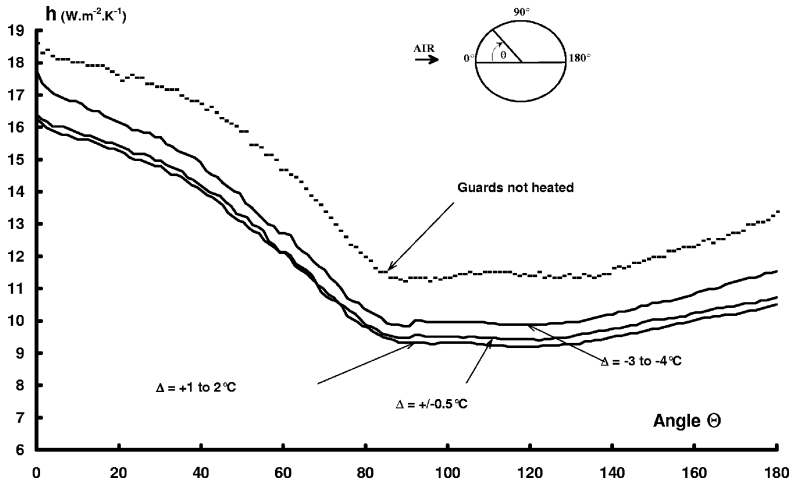


**Figure 3.** Preliminary experiments on a small heated measurement area located at mid-height of the side of the cylinder and sandwiched in between two guard heaters. Distribution of the heat transfer coefficients on the middle line of the measurement area as a function of the angle from the stagnation point and for various fittings $\Delta$ of the guard heaters's temperatures.

be non symmetrical. This was not due to radiation neither to natural convection but to the fact that the guard heaters were slightly different and supplied by two different electrical generators. Thus it was very difficult to fit the two guard heaters exactly at the same temperature. However the very good agreement between experimental and calculated results proves that the experimental profiles were only due to the exchanges by conduction at the surface of the sample.

The effect of these exchanges by conduction on the distribution of the transfer coefficient at the middle line of the measurement area is presented in *figure 3*. The greater the surface conduction was (the more negative the value of $\Delta$), the lower the surface temperatures were and thus the greater the measured transfer coefficient value was. On the contrary, if the temperature of the guard heaters was greater than the temperature of the measurement area ($\Delta = +1°C$ to $+2\,°C$), then the value of the transfer coefficient was apparently smaller. The smaller the transfer coefficient value was, the greater the errors due to surface conduction were, that is they were always more pronounced in the wake. However as soon as the guards were heated and as the difference in temperature $\Delta$ did not exceed a few degrees, the effects of surface conduction on the transfer coefficient at the middle of the measurement area were small. For example, it was shown by calculations that a difference $\Delta$ of $-2\,°C$ in temperature led to a 1% error of the theoretical transfer coefficient value at the stagnation point and a 2% error in the wake.

Previous results concerned the middle line of the measurement area. Errors due to surface conduction could be greater below and above this line, especially in the locations of the measurement area in contact with the guard heaters. These errors in these locations could, in the wake, reach 10–15% of the transfer coefficient value. Thus the effect of surface conduction should have been corrected if one wanted to measure the transfer coefficient everywhere in the measurement area. When the cylinder was in cross flow, correction would have been possible using the calculation procedure described previously. When the cylinder was sloped into the flow fitting the guard heaters and correcting the difference due to surface conduction would have been more difficult and above all some risks of biasing the results could not have been excluded. Hence the idea of coiling a small part of the side of the cylinder and then moving it was abandoned. Despite technical difficulties, the decision was taken to coil most of the cylinder surface.

## 3.4. Making up the final sample

The cylinder ($D = 0.108$ m, $H/D = 3.0$) was made using the same materials and methods as those described previously. It was not totally coiled to lighten the technical work and to respect the limits of the electrical generators. The coiled area corresponded to one tip and to a part of the side of the cylinder (0.20 m in height) adjacent to this tip (*figure 4*). This part was limited by a 0.02 m wide guard heater which has a separate electrical supply.

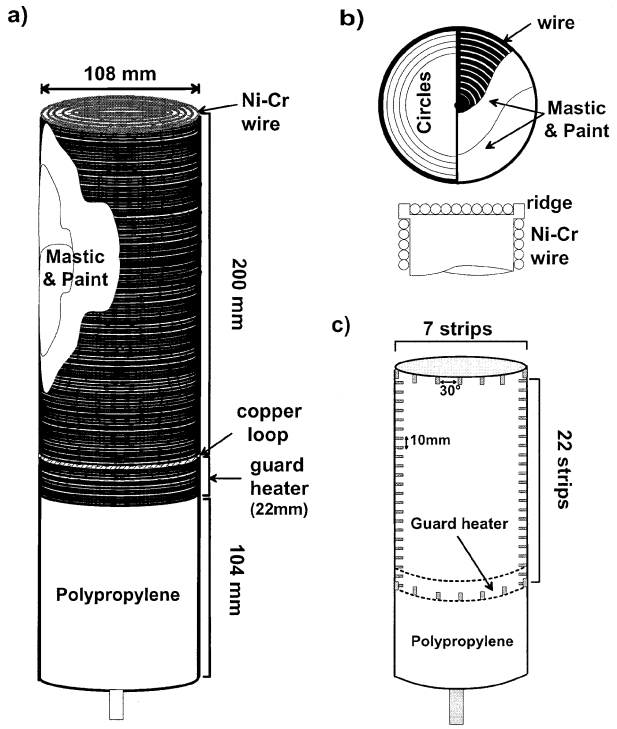


**Figure 4.** How the final sample was made.

Calculations of surface conduction showed its effect was negligible as soon as the distance from the guard heater was greater than 0.015 m. To be on the safe side, only the upper height of the cylinder side (0.150 m from the tip) was considered. Thus measurements on the side of the cylinder were always performed at least 0.04 m away from the guard heater.

The main technical difficulty was continuously coiling the wire on the tip and connecting this part to the wire loops located on the side of the cylinder. To completely cover the tip surface, the wire was coiled in a spiral from the centre of the polypropylene disk to its edge. Every loop was pushed and stuck against the previous one following concentric circles engraved on the disk. Thanks to these engraved circles, the coil did not move off centre and the last loop of the wire matched the edge of the disk perfectly. At this edge, a small 0.1 mm thick and 0.8 mm high ridge (the same height as the diameter of the wire) in the polypropylene disk maintained the spiral coil in place (*figure 4(b)*). This ridge was slit afterwards to let the wire cross through it and to be able to go on coiling the side of the cylinder. Then the surface of the cylinder was covered with mastic and black paint as in the case of the preliminary sample.

In the last stage 1 mm wide aluminium strips were stuck at regular interval along the perimeter and height of the cylinder side (*figure 4(c)*). These strips had a low emissivity and were used as markers during the treatment of the infrared pictures. Seven strips were positioned on the perimeter of the cylinder and twenty two along its height.

## 4. ACQUIRING AND TREATING THE INFRARED PICTURES

### 4.1. Acquiring the infrared pictures

*Figure 5* presents the experimental apparatus. To take the infrared pictures, one of the walls of the experimental cell was replaced by a window made of a $10^{-3}$ m thick polyethylene film. This material was chosen because preliminary studies had shown that it was the most transparent to infrared radiations in the range of wave lengths capture by the camera (2 μm–10 μm). However taking pictures through this window of the surface of a sample of unknown emissivity and which was subjected to a non characterised environment of infrared radiation made it absolutely necessary to have an *in-situ* control of the camera response [25].

To control the response of the camera, a reference target was built. It was made from an aluminium plate ($0.22 \times 0.20 \times 0.02$ m) covered on its two main sides by a continuous coil of a varnished copper wire. A flat PT100 probe was stuck under the coil to measure the reference temperature. The thermal contact between the plate and the probe was made using epoxy resin loaded 80% with an aluminium powder. The copper coil was covered by the same number of coats of mastic and black paint as the sample. Thus the target and the sample had the same emissivity. As the material used to build the target (aluminium and copper) was very thermally conductive, the surface temperature around the PT100 probe was uniform at $\pm 0.5\,^{\circ}$C.

Before each set of experiments, the target was positioned in the experimental cell in place of the sample and the copper wire was supplied with an electrical current. Pictures were taken by the camera (emissivity button tuned to 1.0) in the part of the target surrounding the PT100 probe where the temperature was uniform. The difference between the average values given by the PT100 probe and by the camera was recorded. Results proved that between 50 °C and 80 °C—which corresponded to the range of temperature existing at the

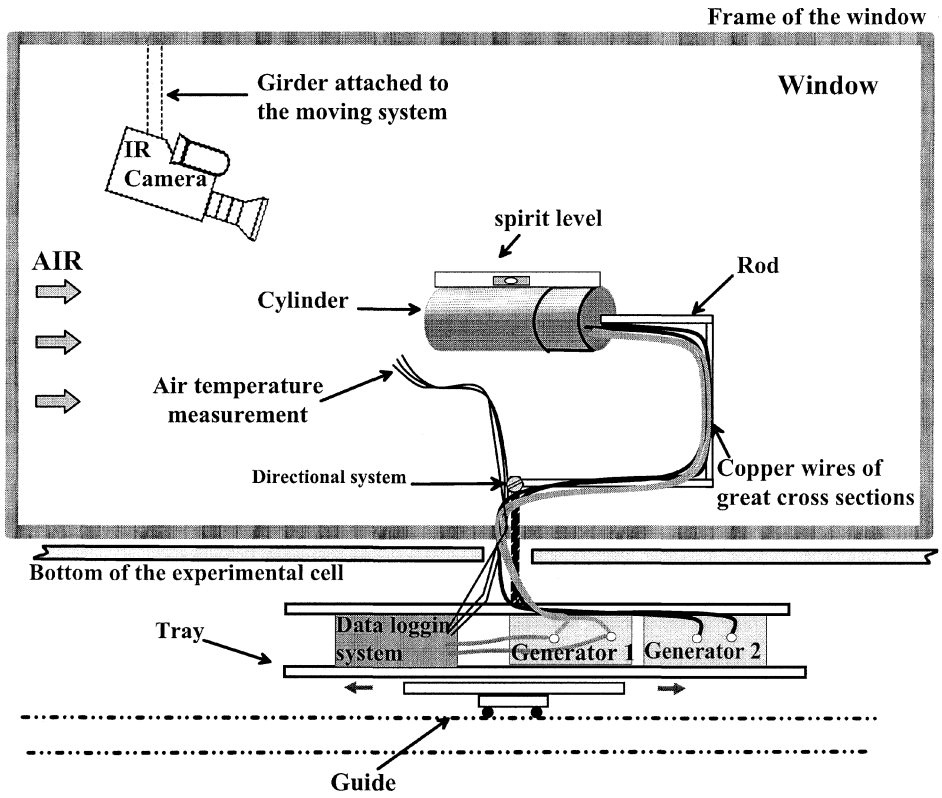


**Figure 5.** Schematic representation of the experimental apparatus. The infrared camera is located outside the experimental cell and separated from the inside by a polyethylene window $10^{-3}$ m in thickness.

surface of the sample during the measurement of transfer coefficients—the response of the infrared camera was 5 °C to 7 °C lower than the temperature recorded by the PT100 probe.

Two of the main causes which could explained this discrepancy were: the unknown surface emissivity of the sample and the temperature gradient which could exist through the surface coat made of mastic and paint (a third cause could be the absorption of infrared radiations by the polypropylene window).

The surface coat of mastic and paint was very thin 0.3 mm to 0.4 mm. The knowledge of the surface heat flux (about 800 $W \cdot m^{-2}$) and of the conductivity of the mastic and paint ($\lambda$ between 0.6 and 1.5 $W \cdot m^{-1} \cdot K^{-1}$) led to the conclusion that the difference in temperature through this coat was less than 0.5 °C and thus fell in the experimental error. This small difference in temperature through the coat justified the use of the reference target to calibrate the camera.

The real emissivity of the sample remained unknown and its knowledge should have required special experimental set up and skill that were not available at the laboratory. It was however possible to show from calculations that the emissivity should have been equal to 0.87 to explain the temperature difference between the reading of the camera and the PT100 probe. An emissivity of 0.87 was close to values of about 0.92 usually found in literature. However it was difficult to know if the emissivity value of 0.87 was the right one since the difference in temperature between the camera reading and the PT100 probe included some absorption of radiation by the polypropylene window.

Finally it was decided that in our case the must reliable procedure was to correct the measurements of the camera using the calibration curve established from the response of the reference target. This correction of 5 °C to 7 °C was a key point of the measurement of surface temperature and if it had not been taken into account, it would have led to an error on the heat transfer coefficient value greater than 30% of the final result.

During the experiments, the cylinder was positioned in the experimental cell of the wind tunnel and maintained

by a set of rotating rods which were fixed to the bottom of the cell (*figure 5*). It was possible to direct the cylinder using this device with a precision of ±2°. The wires coming from the measurement area and from the guard heater were connected (through other electrical wires of larger section and made of copper) to their separate electrical generators located under the bottom of the cell. During the experiments, the air temperature and the voltage and intensity of the electrical current which circulated into the measurement area were automatically recorded every two minutes. About six hours were necessary to reach the steady-state period. During this period, infrared pictures were taken.

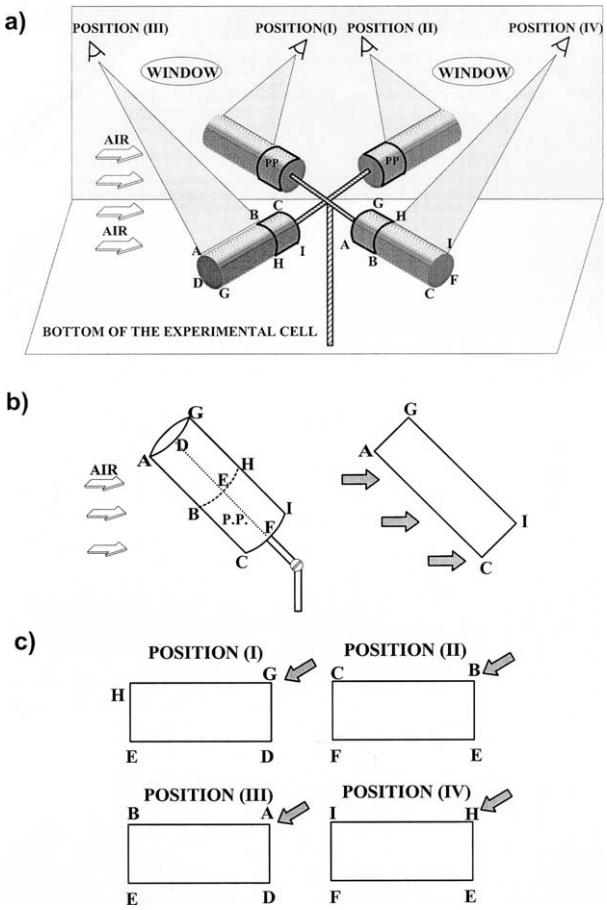


**Figure 6.** Description of how the pictures were taken on the side of the horizontal cylinder sloped at 45° into the flow: (a) experimental positions used to take the 4 pictures; (b) location using letters of the cylinder edges in relation to the flow direction; (c) pinpointing the previous locations on the pictures before piecing them together. The symbol "pp" gives the location of the polypropylene part of the cylinder side which was not coiled.

To map out the whole surface of the cylinder, it was necessary to picture the tips and half of the perimeter of the cylinder side (the distribution of the coefficient was presumed to be symmetrical on the other half of the perimeter). Because of the convexity of the surface, several pictures were needed to map out the side of the cylinder. The cylinder was positioned vertically in the experimental cell only when we had to picture its side for a cross-flow position. In the other cases, that is to picture the tips or to picture the side when it was sloped into the flow, the cylinder had to be placed horizontally.

Mapping out the side of the cylinder sloped at 45° in the flow direction was the most difficult case because it required associating pictures taken on the cylinder placed in four different ways in the experimental cell. *Figure 6* describes the procedure followed in this case to reconstitute the image of the half perimeter "A-G-C-I" (*figure 6 (a)* and *(b)*).

Each of the four positions of the cylinder in the experimental cell led to a different picture of the cylinder side (*figure 6(a)–(c)*). In these pictures, the letters from A to I represented the location of the cylinder edges in relation to the flow direction. The letters B and H separated the heated from the non heated area. As in each of the four positions of *figure 6(a)*, the physical edges had different roles in relation to the flow direction, the four complementary pieces of the complete image could be obtained. We simply had to piece together the pictures (letter by letter) to reconstitute the image "A-G-C-I" (*figure 6(a)–(c)*).

## 4.2. Picture processing

Each picture led to a matrix whose size was 100 by 256 pixels (video format). These pictures were distorted and incomplete and thus had to be corrected and combined. Correcting the distortions was necessary: (1) to be able to interpret visually the images and (2) to calculate exactly the average value of the transfer coefficient. The computer programs used to treat the pictures were developed using the software matlab (version 5.2) completed by its special functions for image processing ("image processing toolbox"). Two cases are given here as examples to illustrate the treatment procedure: (1) on tips (2) on the side of the cylinder sloped at 45° into the flow.

### Treatment of the tips

In spite of some specific problems, such as interactions between the temperature of the sample and of the background, the treatment of the tips was simpler than

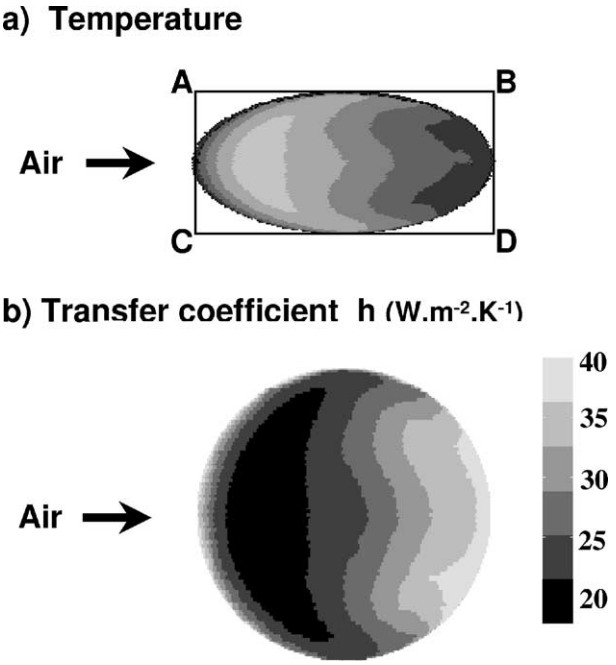


**Figure 7.** Treatment of the picture of a tip: (a) elliptical distorted picture of the temperature on the tip; (b) final map out of the transfer coefficient after correction of the distortion.

the treatment of the side because: (i) the image of a tip came from only one picture, and (ii) the surface of the tips was flat. The video format (100 × 256 pixels) of the picture distorted the circular shape of the tip into an elliptical shape (*figure 7(a)*). This distortion (hereafter called flat distortion) was not only due to the format of the picture (which would have led to a distortion ratio of 2.56) but it integrated the optical characteristics of the camera (external and internal lenses) and the parameters linked to the position of the camera in relation to the surface of the cylinder (distances, view angle). Since the optical characteristics of the camera were not fully known and since the camera/cylinder position changed from one experiment to the other, the distortion ratio had to be calculated for each treatment.

In the first stage, the vertices (ABCD) of the rectangle in which the elliptical outline was inscribed were determined by intersecting the lines which were tangent to the extreme points of the major and minor axis of the ellipse (*figure 7(a)*). The coordinates of these vertices were used to calculate: (1) the slope of the elliptical outline into the picture and (2) the ratio of the flat distortion (major to minor ratio of the ellipse) which afterwards made it possible to restore the circular geometry of the tip.

The temperature measured on the outline of the tip was subjected to two types of error: (1) the effects of treatment during the previous correction of distortion and (2) the proximity of the background. The error due to the proximity of the background was due to the fact that the pixels that were located on the outline of the picture of the tips were sensitive to the temperature of both the tip and the background.

The modulation transfer function of the camera could have been used to localise accurately the border of the sample and to correct the effect of the background. Unfortunately this function remained unknown to us as were some other characteristics of the camera.

Thus pictures were analysed by turning the camera around its optical axis proved that the treatment did not affect the result at a distance of 3 pixels from the outline of the tip. Further than 3 pixels, the effect due to the proximity of the background also seemed to be negligible. Thus it was this internal part of the image which was retained for calculating the heat transfer coefficients and for analysing their distribution on the tips of the cylinder (*figure 7(b)*).

## Treatment of the side

The treatment of the side of the cylinder was more complex than the treatment of its tips because: (1) pictures were subjected to additional geometric distortions due to the convexity of the surface and (2) each of the pictures had to be treated separately and then put together with the others to obtain the complete image.

Convexity of the cylinder surface introduced a geometric distortion of the picture. However its effect on the determination of the transfer coefficient was probably very small. Preliminary experiments had shown that the measurement of temperatures were not affected by the surface curvature as long as the angle between this surface and the optical axis of the camera did not exceed 45°. Moreover as the image of the side of the cylinder contained at least 20 000 values the dimension of a pixel was about 1 mm ×1 mm and its curvature very small. Thus pixel curvature had most probably a negligible effect on the local determination of the transfer coefficient.

The different stages of treatment are presented schematically in *table I*. The way the image of the side of the cylinder sloped at 45° into the flow was rebuilt from the 4 initial pictures taken according to *figure 6* is shown in *figure 8(a)*.

After having checked that the slope of the object in the picture was nil and after having eliminated most of the picture background, pictures I and IV were flipped upside down (*figure 8(a)*). Then the physical markers (aluminium strips) had to be located on each of the four pic-

TABLE I
Schematic representation of the different stages leading to the complete map out of the heat transfer coefficient on the side of the cylinder.

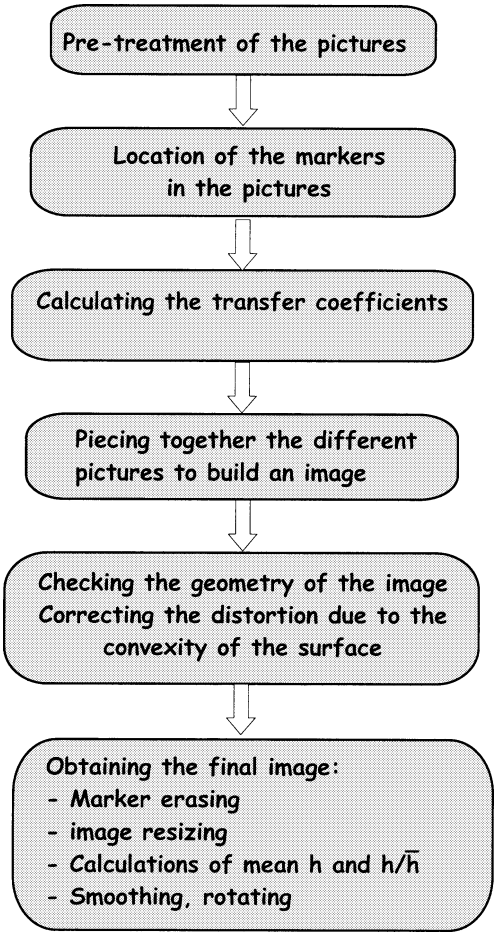


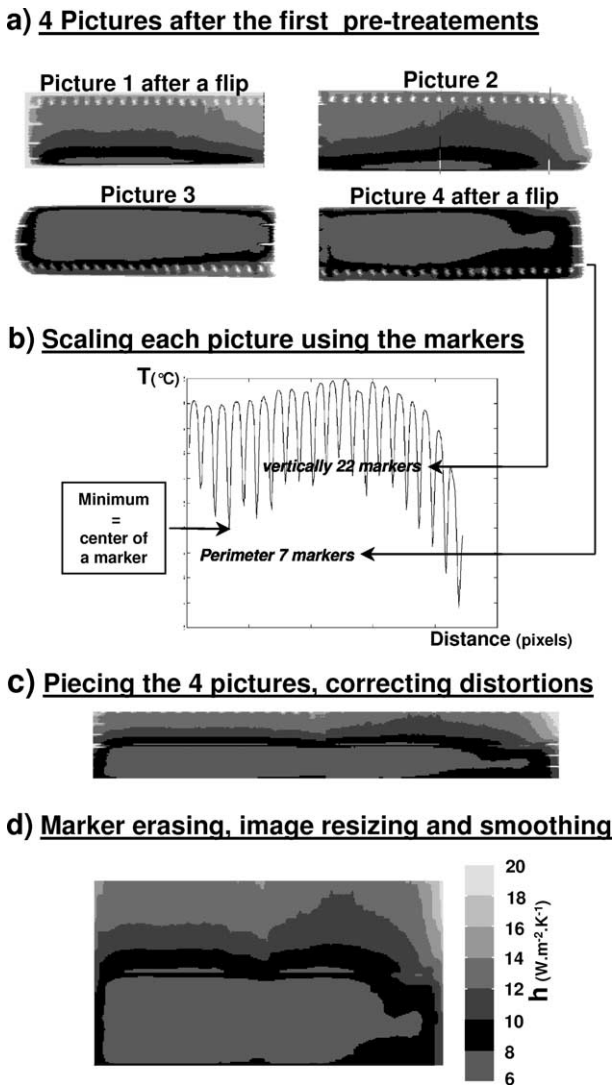


**Figure 8.** Treatment of the pictures on the side of the cylinder sloped at 45° into the flow: (a) 4 pre-treated initial pictures; (b) example of a temperature profile used to locate the markers; (c) complete image after having pieced together the 4 preceding pictures and corrected the distortions due to the convexity of the surface; (d) image after marker erasing and geometrical resizing.

tures. Two temperature profiles were established on two lines (one line in the perimeter direction, the other in the height direction) intersecting the markers (*figure 8(b)*). A computer program automatically researched the coordinates of these markers and provided a precise location and scaling of the picture in relation to the geometry of the sample.

Afterwards, transfer coefficients were calculated and pictures were resized, cut and pieced together to obtain the complete image of the side of the cylinder. Before combining the pictures, the transfer coefficient values in the overlapping regions of the 4 pieces were compared to check that the differences did not exceed the experimental errors (5% of the transfer coefficient value). The combined image of the transfer coefficient distribution on the side of the cylinder sloped at 45° into the flow is shown in *figure 8(c)*.

The coordinates of the markers were located again on the combined image to check that everything was normal and to correct the distortion due to the convexity of the surface of the cylinder. The projection onto a plane (the picture) of markers equally distributed on the surface of half a circle tends to reduce artificially the distance in between the markers located at the two extremities

TABLE II
Distance measured on the image in between the 7 markers positioned regularly on half the perimeter of the cylinder.

| Space between 2 markers | 1–2 | 2–3 | 3–4 | 4–5 | 5–6 | 6–7 |
|---|---|---|---|---|---|---|
| Distance in pixels | 7 | 9 | 7 | 6 | 10 | 8 |

of the semicircle. As for the flat distortion, it was impossible to calculate directly the ratio of distortion due to the convexity of the surface because several optical characteristics of the camera were combined with geometric principles. Thus the distortion ratios were determined *a posteriori* by measuring the distance between the seven markers on the pictures (*table II*). The greater distances were always located in between markers 2 and 3 and between markers 5 and 6 (*table II*). These spaces corresponded to the middle of each of the 2 images which spanned a quarter of perimeter (*figure 8(a)*, pictures (1) + (2), and pictures (3) + (4)). On the edges of these images, distances were smaller. The maximum difference in the distance between two spaces was about 4 pixels (about $6{\cdot}10^{-3}$ m). The distortion was corrected by resizing the different parts of the image located in between two markers to ensure afterwards an equal distance between them.

The last treatments led to the final map out. Markers were erased by interpolation between the nearest region using a special routine. Then the global image was resized to restore the real geometrical proportions of the sample (*figure 8(d)*). Erasing markers and resizing the cylinder made it possible to calculate correctly the mean transfer coefficient value. Mean transfer coefficient values were obtained by averaging all the local values (more than 20 000 pixel values) corresponding to the examined part of the sample (either the side or tips). Then the image could also be smoothed and rotated to improve the visualisation and analysis of the results (*figure 9*).

The final map out of the side and tips of the cylinder either sloped at 45° into the flow or in cross flow position are presented in *figures 9* and *10*, respectively. When the cylinder was in cross-flow, the distribution of the transfer coefficient on the line located mid-height could be compared to the results in the literature obtained by other experimental methods. On average, present results did not differ by more than 5% from those in the literature [29]. Due to the lack of literature, it was impossible to make such a comparison when the cylinder was sloped at 45° into the flow. For the same reason, a direct comparison of the present mapmakings with results in the literature has not been possible.

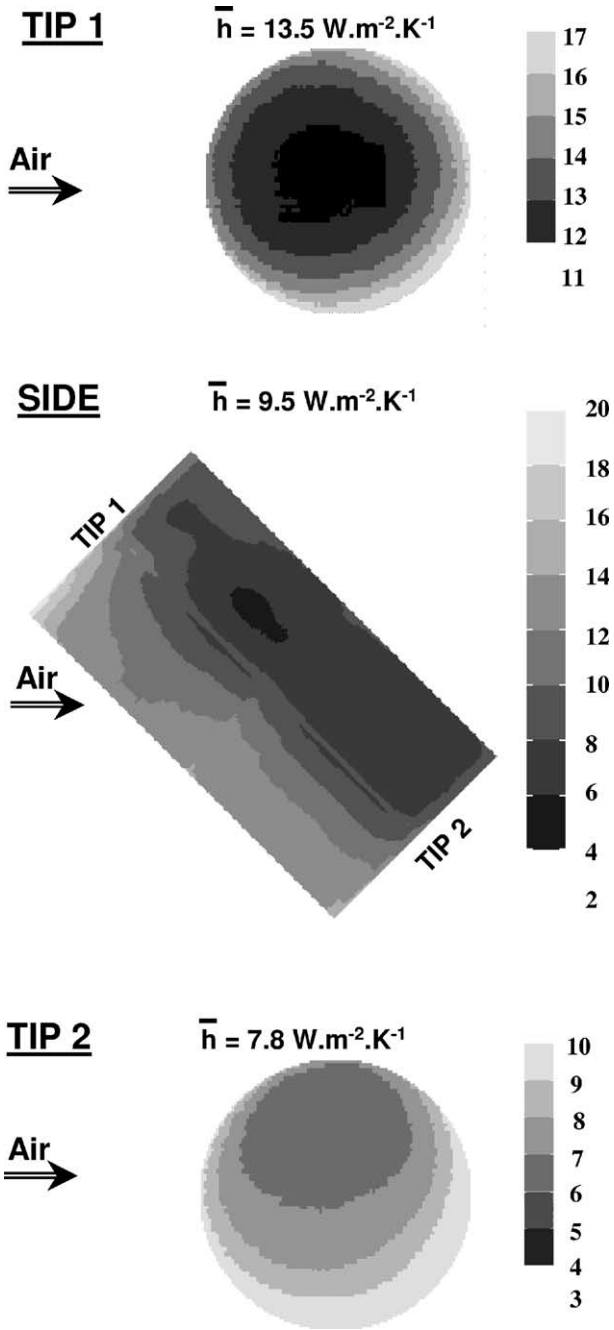


**Figure 9.** Final complete map out of the transfer coefficient at the surface of the cylinder sloped at 45° into the flow, $U = 0.69$ m·s$^{-1}$, $Tu = 1.5\%$.

Observing the images shows that they obey a left to right organisation which is closely linked to the development of the boundary layers at the surface of the cylinder. However in *figure 9(Tip 2)* there is also an organisation

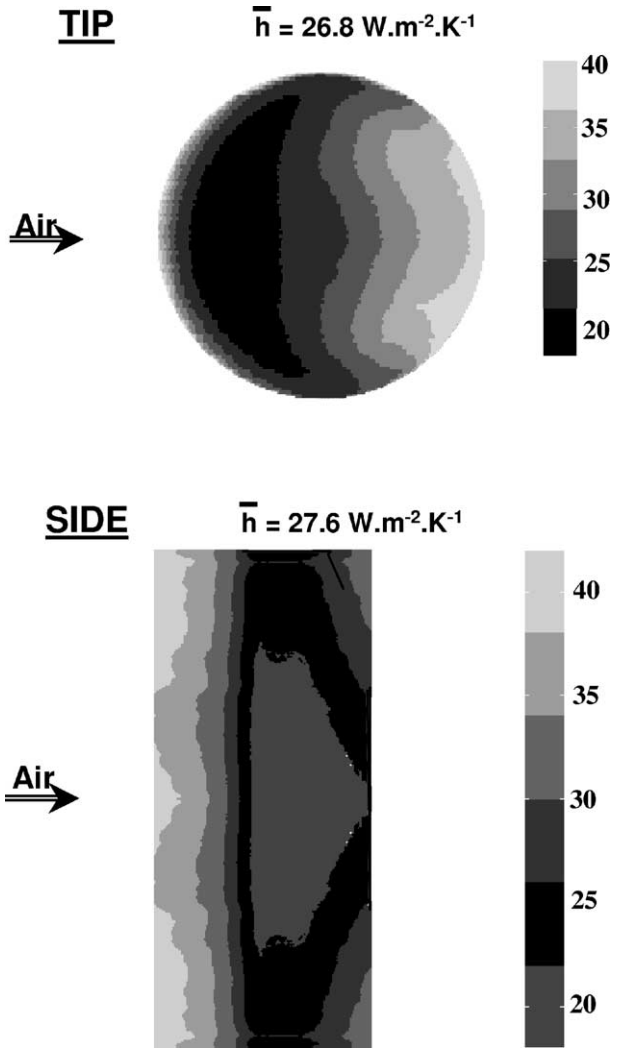


**Figure 10.** Final complete map out of the transfer coefficient at the surface of the cylinder in cross flow, $U = 3.85$ m·s$^{-1}$, $Tu = 1.5\%$ (in this case, coefficient values are the same on both tips).

from the top to the bottom of the image which is probably due to some effects of free convection. This vertical organisation disappears as soon as forced convection is greater, that is, as soon as the convective heat transfer coefficient is greater than about 10 W·m$^{-2}$·K$^{-1}$. In practice, the effect of free convection can easily be decreased by decreasing the temperature at the surface of the sample. However these decrease must be reasonable to keep the result sufficiently precise.

Some other features of the mapmakings can seem curious as for example the presence on the side of the cylinder of a central region where transfer coefficient was minimum. As this minimum area was seen in the partial pictures which had been used to obtain the final image it was not an artefact coming from image processing. Was it due to a defect of the sample? No it was not, because it moved when the cylinder was sloped from 45° to a position parallel to the flow direction. Thus the existence of this minimum was really due to the boundary flow which developed at the cylinder surface. A more detailed interpretation of *figures 9* and *10* would require a detailed analysis of the development of the boundary flow. This goes beyond the limits of this paper and will not be discussed here.

## CONCLUSION

The constant wall heat flux method has the advantage of being based on a simple principle and provides an accurate reference measurement of the distribution of the heat transfer coefficient at the surface of the sample. However this method is difficult to use to map out completely the transfer coefficient at the surface of a cylinder. Because of surface conduction, a quasi-complete coiling of the body surface is required which is in practice very difficult. Moreover measuring the temperatures at the surface of a convex body through a window using an infrared camera is delicate, especially when the body is sloped into the flow. In this case, the complete map out of the transfer coefficient value at the cylinder surface requires complex procedures both to take the pictures and afterwards to treat them.

### *Acknowledgements*

The authors thank A. Lasteyras, J.M. Auberger and F. Peyrin for their technical collaboration and Christine Young for the revision of the English manuscript.

## REFERENCES

[1] Arce J., Sweat V., Survey of published heat transfer coefficients encountered in food refrigeration process, Trans. ASHRAE 86 (1980) 235–260.

[2] Kondjoyan A., Daudin J.D., Determination of transfer coefficients by psychrometry, Internat. J. Heat Mass Tran. 36 (1993) 1807–1818.

[3] Sun S.H.R., Marrero T., Experimental study of simultaneous heat and moisture transfer around single short porous cylinders during convection drying by a psychrometry method, Internat. J. Heat Mass Tran. 39 (1996) 3559–3565.

[4] Ranz M., Marshall W.R., Evaporation from drops: I and II, Chem. Engng. Prog. 48 (1952) 141–151.

[5] Evnochides S., Thodos G., Simultaneous mass and heat transfer in the flow gases past single spheres, AIChEJ 7 (1961) 78–80.

[6] Kondjoyan A., Daudin J.D., Effects of free stream turbulence intensity on heat and mass transfers at the surface of a circular cylinder and an elliptical cylinder, axis ratio 4, Internat. J. Heat Mass Tran. 38 (1995) 1735–1749.

[7] Kondjoyan A., Daudin J.D., Heat and mass transfer coefficients at the surface o f a pork hindquarter, J. Food Engng. 32 (1996) 225–240.

[8] Kestin J., Wood R.T., The influence of turbulence on mass transfer from cylinders, Internat. J. Heat Mass Tran. 93 (1971) 321–327.

[9] Rowe P.N., Claxton K.T., Lewis J.B., Heat and mass transfer from a single sphere in a extensive flowing fluid, Trans. Instn. Chem. Engrs. 43 (1965) 14–32.

[10] Sparrow E.M., Geiger G.T., Local and average heat transfer characteristics for a disk situated perpendicular to a uniform flow, J. Heat Tran. 107 (1985) 321–326.

[11] Smith R.E., Nelson G.L., Henrickson R.L., Analyses on transient heat transfer from anomalous shapes, Trans. ASAE 10 (1967) 236–245.

[12] Succar J., Hayakawa K.I., A response surface method for the estimation of convective and radiative heat transfer coefficients during freezing and thawing of foods, J. Food Science 51 (1986) 1314–1322.

[13] Cleland A.C., Earle R.L., A new method for prediction of surface heat transfer coefficients in freezing, Bull. IIF 1 (1976) 361–368.

[14] Arce J., Modelling beef carcass cooling using a finite element technique, Trans. ASAE 26 (1983) 950–960.

[15] Pham Q.T., Merts I., Wee H.K., Prediction of temperature changes in lamb loins by the finite element method, in: Proceedings of 18$^{th}$ International Congress of Refrigeration, Montreal, Canada, Vol. 4, 1991, pp. 1859–1862.

[16] Achenbach E., Total and local heat transfer from a smooth circular in cross flow at high Reynolds number, Internat. J. Heat Mass Tran. 18 (1974) 1387–1396.

[17] Sogin H.H., A summary of experiments on local heat transfer from the rear of bluff obstacles to a low speed airstream, Trans. ASME 86 (1964) 200–202.

[18] McCormick D.C., Test F.L., Lessmann R.C., The effect of free stream turbulence on heat transfer from a rectangular prism, J. Heat Tran. 106 (1984) 268–275.

[19] Yardi N.R., Sukhatme S.P., Effects of turbulence intensity and integral length scale of a turbulent free stream on forced convection heat transfer from a circular cylinder in cross flow, in: 6$^{th}$ Internat. Heat Transfer Conf., Toronto, Canada, Vol. 5, 1978, pp. 347–352.

[20] Kestin J., Maeder P.F., Sogin H.H., The influence of turbulence on the transfer of heat to cylinders near the stagnation point, J. Appl. Math. Phys. 12 (1961) 115–132.

[21] Ota T., Aiba S., Tsuruta T., Kaga M., Forced convection heat transfer from an elliptic cylinder of axis ratio 1:2, Bull. JSME 26 (1983) 262–267.

[22] Akino N., Kunugi T., Ichimiya K., Mitsushiro K., Ueda M., Improved liquid-crystal thermometry excluding human color sensation, J. Heat Tran. 111 (1989) 558–565.

[23] Stasiek J., Mikielewicz J., Collins M.W., A new method of heat transfer coefficient measurements by liquid crystal and digital processing, Chem. Engrg. Res. Design Part A 75 (1997) 657–662.

[24] Balageas D.L., Bosher D.M., Déom A.A., Fournier J., Gardette G., Application de la thermographie infrarouge passive et stimulée à la mesure des flux thermiques en soufflerie, La Recherche Aérospatiale 4 (1991) 51–72.

[25] Gaussorgues G., La Thermographie Infrarouge, 3$^{ème}$ ed., Lavoisier, Paris, 1989.

[26] Meinders E.R., Van der Meer Th.H., Lasance C.J.M., Application of infrared thermography to the evaluation of local convective heat tranfer on arrays of cubical protusions, Internat. J. Heat Fluid Flow 18 (1997) 152–159.

[27] Kondjoyan A., Boisson H.C., Comparison of calculated and experimental heat transfer coefficients at the surface of circular cylinders placed in a turbulent cross-flow of air, J. Food Engng. 34 (1997) 123–143.

[28] Ozisik N.M., Heat Transfer a Basic Approach, McGraw-Hill, New York, 1985.

[29] Ghisalberti L., Vers une caractérisation rapide des échanges de chaleur et de matière entre l'air et les produits alimentaires solides, Thèse de Doctorat de l'ENSIA (France), 2000.